DOI: 10.1002/adsc.200800424

Palladium Nanoparticles in Allylic Alkylations and Heck Reactions: The Molecular Nature of the Catalyst Studied in a Membrane Reactor

Montserrat Diéguez,[a,*] Oscar Pàmies,[a] Yvette Mata,[a] Emmanuelle Teuma,[b] Montserrat Gómez,[b,*] Fabrizio Ribaudo,[c] and Piet W. N. M. van Leeuwen[c,d,*]

[a] Departament de Química Física i Inorgànica. Universitat Rovira i Virgili. Campus Sescelades, C/Marcel·lí Domingo, s/n. 43007 Tarragona, Spain
Fax: (+34)-97-755-9563; e-mail: montserrat.dieguez@urv.cat
[b] Laboratoire Hétérochimie Fondamentale et Appliquée, UMR CNRS 5069. Université Paul Sabatier. Bât 2R1, 2ième étage, 118, route de Narbonne. 31062 Toulouse cedex 9, France
Fax: (+33)-56-155-8204; e-mail: gomez@chimie.ups-tlse.fr
[c] van't Hoff Institute for Molecular Sciences, University of Amsterdam, Nieuwe Achtergracht 166, 1018 WV Amsterdam, The Netherlands
Fax: (+34)-97-792-0224; e-mail: pvanleeuwen@iciq.es
[d] Institute of Chemical Research of Catalonia (ICIQ), Av. Països Catalans 16, 43007 Tarragona, Spain

Received: July 9, 2008; Revised: September 22, 2008; Published online: November 4, 2008

Supporting information for this article is available on the WWW under http://dx.doi.org/10.1002/adsc.200800424.

Abstract: A series of palladium nanoparticles stabilized by five chiral sugar-based oxazolinyl-phosphite ligands, containing various substituents at the oxazoline and phosphite moieties has been synthesized. They were characterized by transmission electron microscopy (TEM), X-ray powder diffraction (XRD), infrared spectroscopy (IR) and elemental analysis. These nanoparticles were applied in Pd-catalyzed asymmetric allylic alkylation and Heck coupling reactions. A detailed study to elucidate the nature of the active species using a continuous-flow membrane reactor (CFMR), accompanied by TEM observations, classical poisoning experiments, and kinetic measurements have been carried out. Conclusive evidence of the nature of the species involved in the use of PdNPs in asymmetric catalytic reactions has been obtained. The CFMR experiments proved the molecular nature of the true catalysts and all conversions can be justified by the amount of molecular palladium that leached as measured by ICP-AES.

Keywords: active species; asymmetric catalysis; C–C coupling; nanocatalysts; structure elucidation

Introduction

The chemistry and catalytic properties of metal colloids have attracted increasing interest during the last decade.[1] One important application of metallic nanoparticles (MNPs) may be found in catalysis because of their large surface area and concomitant higher potential activity and because of their recyclability, both of which represent a breakthrough at the frontier between homogeneous and heterogeneous catalysis.[1] In this context, MNPs have proven to be efficient and selective catalysts for several types of catalytic reactions, such as olefin hydrogenation and C–C coupling.[1g] Despite the striking developments of nanocatalysts, their use as enantioselective catalysts is rare and not unexpectedly this remains the area of homogeneous catalysis. Notable examples of MNPs as asymmetric catalysts include: (a) the asymmetric Pt-cinchonidine system for the hydrogenation of ethyl pyruvate,[2] (b) the Pd-BINAP chiral system for the hydrosilylation of styrene,[3] and (c) the enantioselective Pd-diphosphite systems for the allylic alkylation of racemic substrates.[4]

Thus, while the first examples of the use of MNPs as enantioselective catalysts or catalyst precursors have been reported, more research needs to be done for which two main directions can be distinguished. The first goal, not different from molecular homogeneous systems, is the systematic evaluation of the effectiveness of new chiral ligands to study the potential

of nanocatalysts in asymmetric catalysis. Such a task becomes significantly more facile if modular chiral ligands are readily at hand. Carbohydrate-based ligands are one class that is particularly useful for addressing this need.[5] The second research target in asymmetric catalysis using MNPs is to learn whether or not the MNPs are responsible for the catalytic activity, or that molecular species leached from the MNP are the actual catalyst.[6] In general, the nature of the active species has been proposed based on circumstantial evidence such as poisoning of the MNPs (i.e., CS_2, Hg, etc.), TEM observations, kinetic measurements, reaction selectivity and, in some cases,[7] reactivity patterns.[4,6a,h]

The possible involvement of dynamic equilibria between solid palladium (or PdNPs) and dissolved molecular palladium species in palladium-catalyzed coupling reactions has been the subject of much debate. De Vries studied his ligand-free catalyst for the Heck reaction extensively using ES-MS to establish the nature of the catalyst.[8] In addition he reviewed a large number of publications on this matter and concluded that at least for reactions conducted at high temperatures (>130 °C) such equilibria are involved.[6b] Jones and co-workers scrutinized in their review over 500 reports on palladium precursors used in Heck and Suzuki coupling reactions and their conclusions agree with those of the De Vries as regards the solid/colloid/nanoparticle precursors, which leaves the situation undecided for the majority of reported protocols.[6a]

Therefore, it is important to develop a practical experiment that reveals definitively the nature of the true catalyst in the liquid phase. Recently, Rothenberg and co-workers have developed a two-cell membrane batch reactor to probe if molecular palladium species generated by leaching or palladium nanoparticles are the true catalysts in the ligand-free Heck and Suzuki reactions; indications are that metal leaching in the ligand-free system is responsible for the catalytic activity.[9] In the experiment with the two-compartment reactor of Rothenberg et al. nanocolloid particles of 15 nm were used and the reactor contains an alumina membrane having a pore diameter of 5 nm. No enforced flow was applied and movement of the particles from one compartment to the other relied on diffusion; experiments took several days at 100 °C. In view of the size of the nanopores of 5 nm it would seem that palladium nanoparticles as used in this study (2.5 nm) will also pass the alumina membrane, albeit slowly.

This paper describes the use of sugar-based oxazolinyl-phosphite ligands (Figure 1) as a new type of stabilizers for PdNPs in order to facilitate the catalyst recovery and recycling in the enantioselective Pd-catalyzed allylic substitution and Heck coupling reactions. Molecular catalytic precursors containing this ligand

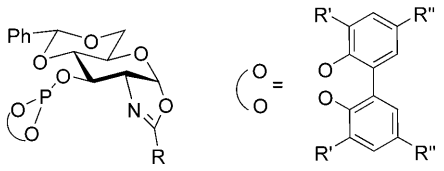

Figure 1. General structure for oxazolinyl-phosphite ligands used in this paper.

series have provided excellent activities and selectivities (regio- and enantioselectivities) for both processes in a wide range of substrate types.[10] In MNPs it is assumed that the phosphite groups of the ligands coordinate firmly to the surface atoms of the nanoparticles and, in addition, the oxygen atoms of the sugar moieties are able to interact weakly with this surface.[4] We also present a detailed study to provide conclusive evidence of the nature of the species involved in the catalytic reaction in liquid phase by introducing the use of a continuous-flow membrane reactor (CFMR), combined with TEM observations, classical poisoning and kinetic measurement experiments. The use of the continuous-flow membrane reactor (CFMR) has been crucial to elucidate the true nature of the catalysts. The CFMR system has a cut-off molecular weight of 700 Dalton and thus it will retain the MNP species, but the mononuclear metal species will pass the membrane.[11] The CFMR system has been used previously for the study of catalyst leaching from dendrimeric catalysts as it retains the dendrimeric species.[12] Especially allylic palladium substitution reactions were found to be prone to metal leaching. The CFMR offers a more accurate yardstick to establish the involvement of molecular species than the two-compartment reactor mentioned above. Furthermore, the reactions in the present study were carried out at a low temperature (T= 23 °C, see below).

Results and Discussion

Synthesis and Characterization of Pd-Nanoparticles Stabilized by Chiral Oxazolinyl-Phosphites

Pd1–Pd5 nanoparticles were prepared from $[Pd_2(dba)_3]$ under hydrogen pressure (3 bar) in the presence of the appropriate chiral ligand **1–5** (ligand-to-palladium ratio 0.2) at room temperature in THF, based on the methodology previously described (Scheme 1).[13] They were isolated by precipitation, washed with dry pentane and dried under reduced pressure. They were found to be stable, both in solution and in the solid state. **Pd1–Pd5** were analyzed by transmission electron microscopy (TEM), X-ray powder diffraction (XRD), infrared spectroscopy (IR) and elemental analysis.

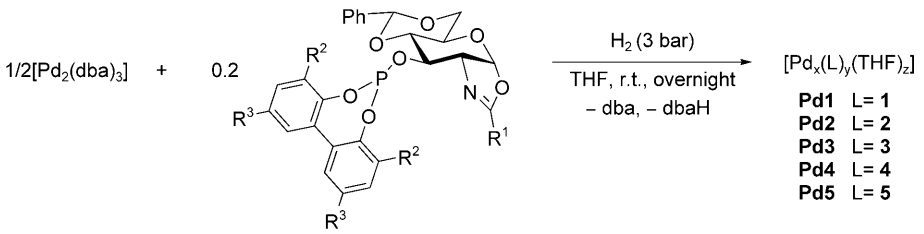

1 R^1 = Ph; R^2 = $SiMe_3$; R^3= H
2 R^1 = Ph; R^2 = R^3 = *t*-Bu
3 R^1 = Me; R^2 = R^3 = *t*-Bu
4 R^1 = *i*-Pr; R^2 = R^3 = *t*-Bu
5 R^1 = *t*-Bu; R^2 = R^3 = *t*-Bu

Scheme 1. Synthesis of **Pd1–Pd5** nanoparticles.

The size and morphology of PdNPs were investigated by TEM analysis (Figure 2). These particles displayed a small spherical shape showing a tendency to give inter-particle organization and in some cases agglomeration regions were observed. The nanoparticle size distribution was estimated from the measurement of about 300 particles, assuming a spherical shape, found in an arbitrary chosen area in enlarged microphotographs (Figure 3). The mean size found for all PdNPs prepared was *ca.* 2.5 nm with a narrow size distribution (Table 1). The concentration of the medium reaction had no effect on the particles size or dispersion (dilution range from 5×10^{-4} to 2.5×10^{-3} mol$\times$L^{-1}, keeping the ligand-to-palladium ratio constant).

In all cases, the X-ray powder diffraction (XRD) showed the face-centered cubic (fcc) packing mode of palladium atoms within the nanoparticle metal core (see Supporting Information). The diameter of the different nanoparticles could also be estimated by means of the Debye–Scherrer equation (using the parameters obtained with Rietveld's refinements).[14] The calculated diameters were between 2.2 and 2.5 nm, in good agreement with TEM observations (Table 1). Palladium oxide was not observed in any case.

IR spectra of PdNPs **Pd1–Pd5** showed bands at 1594–1649 cm^{-1} and 1019–1029 cm^{-1} corresponding to C–N and P–O stretching bands, which are shifted compared to the free ligands (Table 1). This confirms the presence of the oxazolinyl-phosphite ligands at the surface of the particles (see Supporting Information for spectra).

The elemental analyses, C, H, N, P and Pd, of the PdNPs prepared (**Pd1–Pd5**) are shown in Table 2. These analyses indicated a similar Pd/P ratio of *ca.* 15/2 for all the nanoparticles. These elemental analysis together with the diameter data (*ca.* 2.4 nm, Table 1) and packing structure (fcc) of the nanoparticle core are in agreement with a structure similar to that of the $[Pd_{561}(OAc)_{180}(Phen)_{60}]$ giant cluster proposed by Moiseev and co-workers. [The diameter of the MNPs together with the packing structure determines the number of layers and the amount of metal atoms in the cluster. So for instance, a 2.4 nm PdNP with fcc packing structure corresponds to a nanocluster that contains 561 Pd atoms in five layers, while a 3.15 nm PdNP corresponds to a seven-shell cluster that contains 1515 Pd atoms. See for instance ref.[1b]] This full-shell nanocluster contains ~561 Pd atoms in five layers with an icosahedron arrangement and a mean diameter of 2.4 nm.[15,16] Therefore, the outer layer contains ~252 palladium atoms surrounded by 60 ligands coordinated in a bidentate fashion on the palladium atoms located at the vertices (12) and the edges (~48 only, for steric reasons out of a total of 120) of the icosahedron, in a stacked fashion.[17] The present oxazolinyl-phosphite ligand may also coordinate to atoms in edge and vertex positions in a bidentate manner. The oxazolinyl-phosphite ligand is bulkier than phenanthroline, yet our PdNPs show a slightly higher ligand-to-palladium ratio than the Moiseev cluster (75 *vs.* 60 bidentate ligands per cluster of the same size).[18] The reason for this higher ligand-to-palladium ratio is that oxazoline coordinates weakly to zerovalent palladium. Therefore, some or all oxazoline-phosphite ligands may be coordinated as monodentate ligands to palladium atoms located at the faces, the edges and even the vertices of the icosahedron with their phosphorus donor groups.

Application of PdNPs to Asymmetric C–C Bond Formation Reactions

In this section, we present the application of these new PdNPs as catalysts in the asymmetric allylic alkylation and Heck coupling reactions. The interest of these asymmetric C–C bond formation processes is found in their usefulness in organic synthesis allowing the formation of enantioselective carbon-carbon and

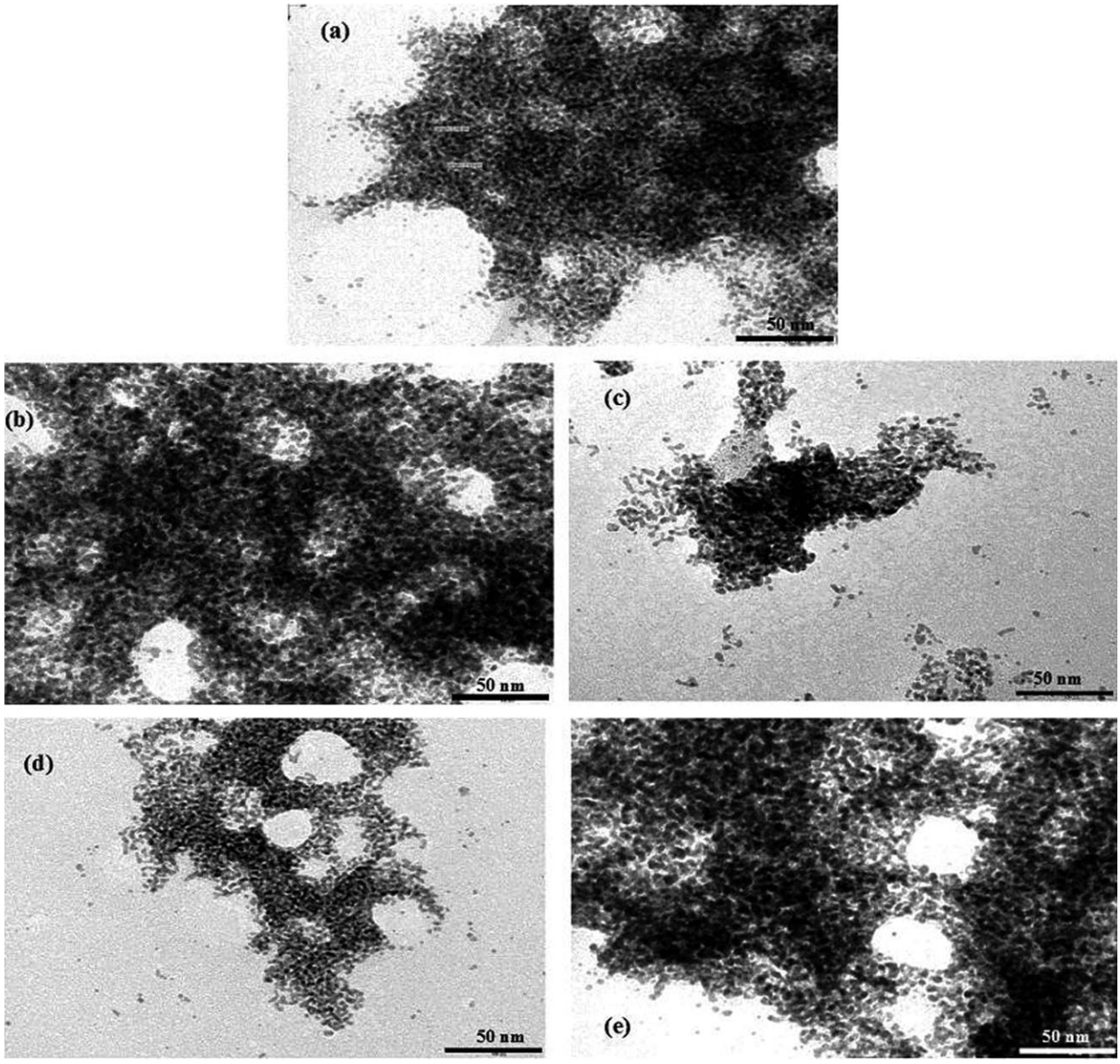

Figure 2. TEM micrographs of PdNPs synthesized in THF from $[Pd_2(dba)_3]$ and in the presence of 0.2 mol% of ligand: (a) **Pd1**; (b) **Pd2**; (c) **Pd3**; (d) **Pd4** and (e) **Pd5**.

carbon-heteroatom bonds under mild reaction conditions.[19]

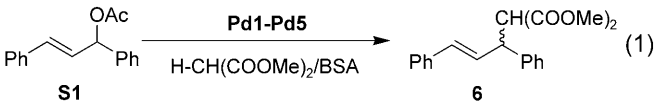

(1)

Asymmetric Pd-Catalyzed Allylic Alkylation of *rac*-3-Acetoxy-1,3-diphenyl-1-propene

Pd1–**Pd5** nanoparticles were used as catalytic precursors in the Pd-catalyzed asymmetric allylic alkylation of *rac*-3-acetoxy-1,3-diphenyl-1-propene **S1**, using dimethyl malonate under basic conditions [Eq. (1)].[20] In a previous work, we studied this catalytic reaction using the corresponding molecular catalytic systems and reaction conditions were optimized for a variety of ligands carrying different donor groups.[10a] Here, we used as starting reaction conditions those that provided the best results with palladium molecular catalysts (i.e., dichloromethane as solvent and room temperature).[10a] The results are summarized in Table 3.

In a first set of experiments, the effect on catalysis of the added ligand was studied using **Pd1** nanoparticles (Table 3, entries 1–4). The results indicated that without the addition of free ligand, the catalytic

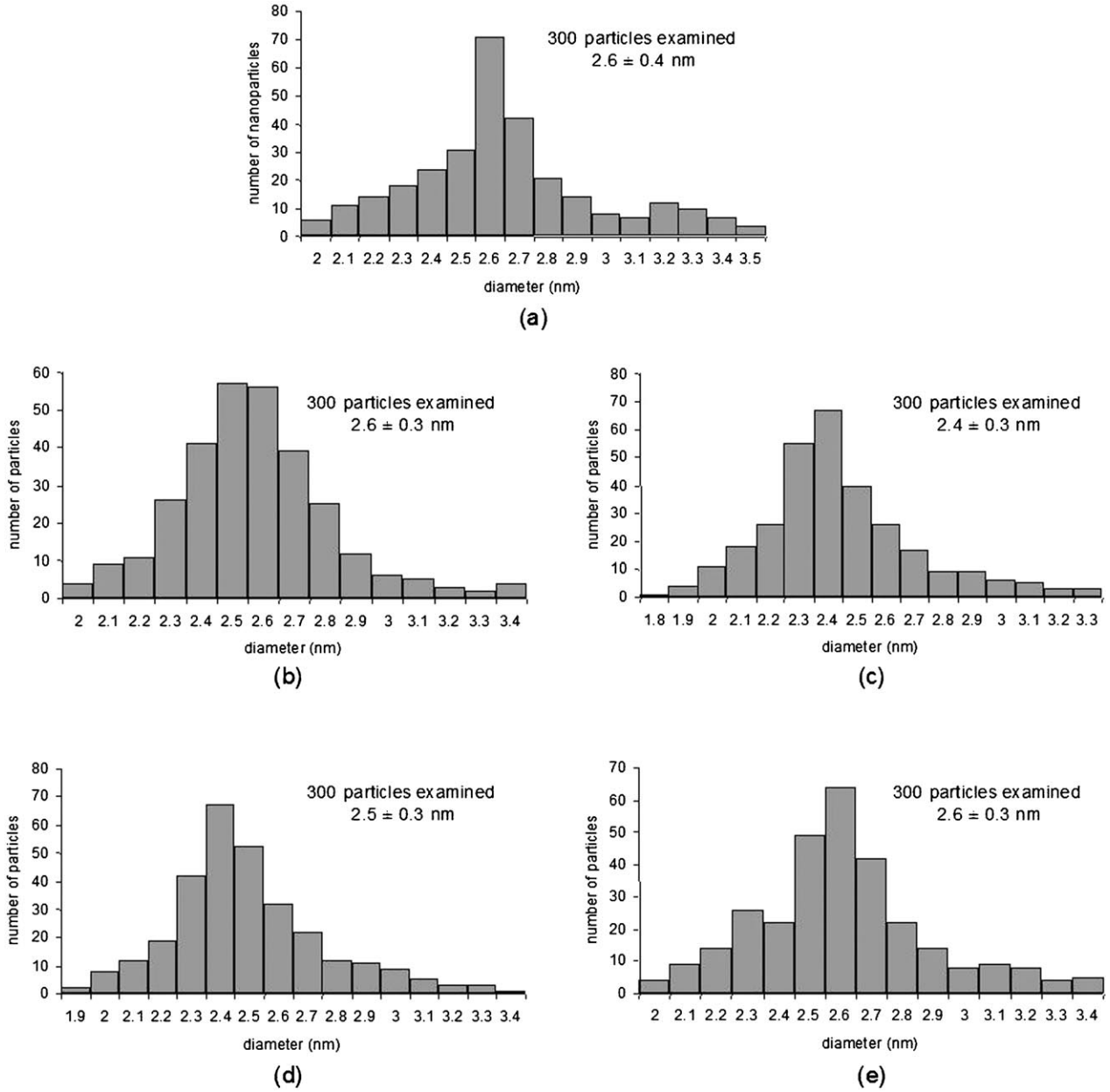

Figure 3. Size distributions obtained from TEM micrographs of PdNPs: (a) **Pd1**; (b) **Pd2**; (c) **Pd3**; (d) **Pd4** and (e) **Pd5**.

Table 1. Diameter and IR data for **Pd1**-**Pd5** nanoparticles and IR data for ligands **1**-**5**.

	Pd1–**Pd5** nanoparticles			Free ligand
Ligand	d(TEM) (nm)	d(XRD) (nm)	IR (cm^{-1})[a]	IR (cm^{-1})[a]
1	2.6 ± 0.4	2.55 ± 0.04	1649 (C=N), 1025 (P−O)	1650 (C=N), 1015 (P−O)
2	2.6 ± 0.3	2.41 ± 0.03	1594 (C=N), 1019 (P−O)	1651 (C=N), 1014 (P−O)
3	2.4 ± 0.3	2.41 ± 0.03	1636 (C=N), 1021 (P−O)	1650 (C=N), 1018 (P−O)
4	2.5 ± 0.3	2.35 ± 0.05	1630 (C=N), 1029 (P−O)	1666 (C=N), 1019 (P−O)
5	2.6 ± 0.3	2.21 ± 0.05	1647 (C=N), 1027 (P−O)	1651 (C=N), 1017 (P−O)

[a] IR spectra recorded in 4000–400 cm^{-1} range as KBr pellets. Only the two more representative absorptions are indicated.

system is practically inactive (Table 3, entry 1), while the addition of small amounts (5–10%) of ligand increases the reaction rate, having little effect on enantioselectivity (Table 3, entries 2 and 3 *vs.* 1), as observed for other related PdNP catalytic systems.[4] This effect may be due to the agglomeration produced

Table 2. Elemental analysis and calculated formula for **Pd1–Pd5**.

Nanoparticle	% C	% H	% N	% P	% Pd	Formula	Idealized formula
Pd1	36.92	4.09	1.02	2.09	43.55	$Pd_{32}(L)_5(THF)_{10}$	$Pd_{561}(L)_{88}(THF)_{173}$
Pd2	36.74	3.74	0.70	1.69	47.60	$Pd_{32}(L)_{3.9}(THF)_8$	$Pd_{561}(L)_{68}(THF)_{140}$
Pd3	36.74	4.89	0.96	1.85	46.30	$Pd_{32}(L)_{4.3}(THF)_{10}$	$Pd_{561}(L)_{75}(THF)_{173}$
Pd4	38.71	4.75	0.78	1.84	45.20	$Pd_{32}(L)_{4.4}(THF)_{10}$	$Pd_{561}(L)_{77}(THF)_{173}$
Pd5	37.45	4.32	0.84	1.85	45.42	$Pd_{32}(L)_{4.3}(THF)_{8.5}$	$Pd_{561}(L)_{75}(THF)_{149}$

Table 3. Asymmetric Pd-catalyzed allylic alkylation of **S1** using nanoparticle and molecular catalytic systems.

		Nanoparticle precursor[a]			Molecular precursor[b]		
Entry	**L**	**S1/PdL/L**	% Conv.[c] (h)	% *ee* **6**[d]	**S1**/Pd/**L**	% Conv.[c] (h)	% *ee* **6**[d]
1	**1**	20/1/–	<5 (72)	–	100/1/0.9	95 (0.5)	86 (*S*)
2	**1**	20/1/0.05	33 (72)	70 (*S*)	–	–	–
3	**1**	20/1/0.1	60 (72)	71 (*S*)	–	–	–
4	**1**	20/1/0.2	62 (72)	70 (*S*)	–	–	–
5	**2**	20/1/0.1	51 (72)	80 (*S*)	100/1/0.9	100 (0.5)	92 (*S*)
6	**3**	20/1/0.1	32 (72)	60 (*S*)	100/1/0.9	100 (0.25)	85 (*S*)
7	**4**	20/1/0.1	78 (72)	46 (*S*)	100/1/0.9	92 (0.5)	86 (*S*)
8	**5**	20/1/0.1	100 (24)	20 (S)	100/1/0.9	67 (0.5)	45 (S)

[a] 5 mol% Pd, 0.5 mmol of **S1**, 1.5 mmol of BSA, 1.5 mmol of dimethyl malonate, CH_2Cl_2 as solvent, $T=23\,°C$.
[b] 0.5 mol% $[Pd(\mu\text{-}Cl)((\eta^3\text{-}C_3H_5)]_2$, 0.9 mol% of ligand, 0.5 mmol of **S1**, 1.5 mmol of BSA, 1.5 mmol of dimethyl malonate, CH_2Cl_2 as solvent, $T=23\,°C$.
[c] Conversion percentage determined by ^1H NMR.
[d] Enantiomeric excesses determined by HPLC on a Chiralcel-OD column. Absolute configuration shown in parentheses.

under catalytic conditions (corroborated by TEM analysis after catalysis, see Figure 5b) by ligand desorption from the metallic surface when not enough ligand is present in the medium, which leads to a catalytically inactive heterogeneous species. When free ligand is added (see Section: Elucidation of the Active Species) this leads to the formation of molecular, catalytically active palladium species by metal leaching. It should be noted that the addition of larger amounts of ligand (more than 10 mol%) did not increase the reaction rates further (Table 3, entry 4 *vs.* 3). Therefore, addition of 10 mol% of ligand was applied for the subsequent reactions.

We then tested the remaining PdNPs, **Pd2–Pd5**. We found an effect of the size of the oxazoline substituent on the catalytic performance (activity and enantioselectivity). Therefore, activities were higher when more sterically demanding substituents were present (Table 3, entries 3, 5–8), the most active being system **Pd5** which contains a *tert*-butyloxazoline substituent (entry 8, Table 3). However, enantioselectivities decrease when steric hindrance increases (Table 3, entries 3, 5–8). Both catalytic findings contrast with the results of the analogous molecular system (Table 3). This fact can point to a different nature of catalytic species or a different extent of metal leaching (see Section: Elucidation of the Nature of the Active Species). Regarding the biphenyl phosphite moiety, we found a slight but distinct effect on activity and enantioselectivity. Therefore, **Pd2**, stabilized by ligand **2** which contains *tert*-butyl groups at the *ortho* and *para* positions of the biphenyl phosphite moiety, provided better enantioselectivity and slightly lower activities than **Pd1**, containing trimethylsilyl *ortho*-substituted biphenyl phosphite moiety. The same effect was observed for the analogous molecular systems. In summary, good enantioselectivities (*ee*s up to 80%) with low activities were obtained with **Pd1** and **Pd2** nanoparticle catalytic systems. If we compare the results obtained with the application of the nanoparticles with the ones obtained with the molecular systems, we observed that the nanoparticles are less active and less enantioselective than their corresponding homogeneous catalysts (Table 3).

For the best PdNPs with regard to asymmetric induction, **Pd1** and **Pd2**, we next studied catalyst recycling (Figure 4).[21] Interestingly, the nanoparticles could be reused three times maintaining the enantioselectivity, but with decreases in activity.[22] This observation may point to metal leaching from the nanoparticles (see Section: Elucidation of the Nature of the Active Species) or to blocking of the solid catalyst by strongly adsorbing species.

Asymmetric Pd-Catalyzed Phenylation of 2,3-Dihydrofuran

Pd1–**Pd5** were also used as catalyst precursors in the asymmetric Heck reaction of 2,3-dihydrofuran **S2** and

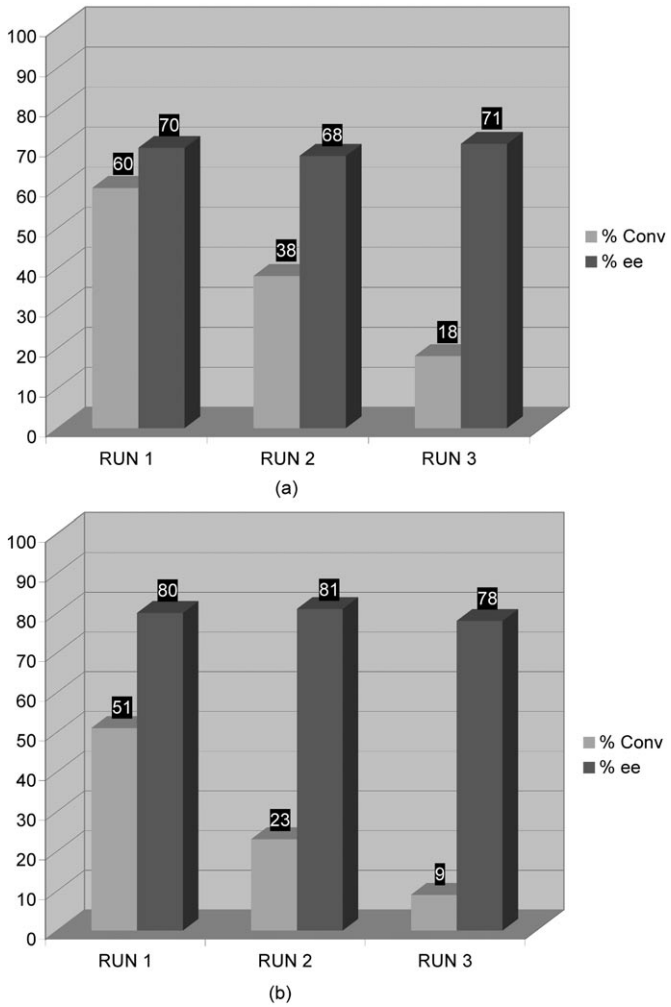

Figure 4. Catalyst recycling for the asymmetric allylic alkylation of **S1** using: (a) **Pd1** and (b) **Pd2**.

phenyl triflate [Eq. (2)] as a model reaction. For this process, not only does the enantioselectivity of the process need to be controlled but regioselectivity is

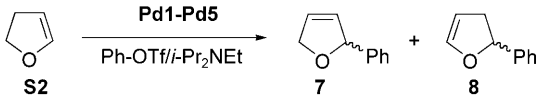

(2)

also a problem because a mixture of regioisomers can be obtained. The reactions were carried out by adding 10 mol% of the corresponding ligand to the nanoparticle suspension under the reaction conditions that provided the best results with the molecular system [i.e., THF as solvent, 50 °C and $(i\text{-Pr})_2$NEt as base].[10b,c] The results are summarized in Table 4.

Pd1–Pd5 systems show low activity (conversions up to 23% after 72 h of reaction), but they provided good regio- (up to 82%) and enantioselectivities (up to 68%). We also found an effect of the size of the oxazoline substituent and the substituents at the biphenyl phosphite moiety in the catalytic performance (activity and selectivity); when the size of the group on the oxazoline decreased, the regio- and enantioselectivity of the catalyst increased (Table 4, entries 1–5). Moreover, the presence of trimethylsilyl *ortho*-substituted biphenyl phosphite moiety has a positive effect on activity and enantioselectivity (Table 4, entries 1 *vs.* 2). In contrast to that observed in the allylic alkylation, these results follow the same trend as that observed for the comparable molecular systems. The best results were obtained with **Pd1** and **Pd3** nanoparticle catalysts. **Pd3** was reused once without significant loss in activity and selectivity (Table 4, entries 3 and 6). As observed for the allylic alkylation of **S1**,

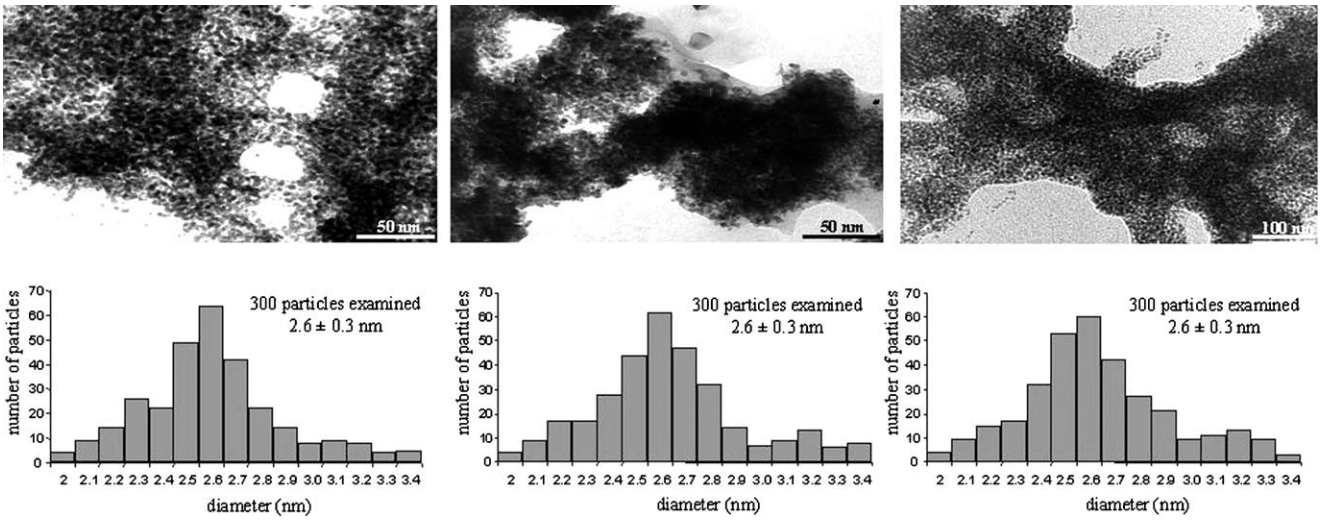

Figure 5. TEM micrographs showing **Pd5** nanoparticles: (a) before catalysis, (b) after the allylic alkylation of **S1** and (c) after allylic alkylation of **S1** and washed five times with THF.

Table 4. Asymmetric Pd-catalyzed phenylation of **S2** using nanoparticle and molecular catalytic systems.

		PdNP precursor[a]			Molecular precursor[b]		
Entry	Ligand	% Conv.[c] (h)	**7**/**8**[c]	% *ee* **7**[c]	% Conv.[c] (h)	**7**/**8**[c]	% *ee* **7**[c]
1	**1**	23 (72)	81/19	65 (*R*)	100 (15)	97/3	99 (*R*)
2	**2**	17 (72)	76/24	63 (*R*)	98 (24)	87/13	97 (*R*)
3	**3**	19 (72)	82/18	68 (*R*)	94 (24)	97/3	99 (*R*)
4	**4**	15 (72)	64/36	54 (*R*)	80 (24)	71/29	84 (*R*)
5	**5**	8 (72)	52/48	55 (*R*)	12 (24)	65/35	83 (*R*)
6[d]	**3**	15 (72)	82/18	68 (*R*)	–	–	–

[a] 10 mol% Pd, 2 mmol of **S2**, 0.5 mmol of PhOTf, 1 mmol of $(i\text{-Pr})_2$NEt, THF as solvent, $T=50\,°C$, 10 mol% of ligand added.
[b] 1.25 mol% of $[Pd_2(dba)_3]$, 2 mmol of **S2**, 0.5 mmol of PhOTf, THF as solvent, 1 mmol of $(i\text{-Pr})_2$NEt, $T=50\,°C$.
[c] Conversion percentages based on PhOTf and enantiomeric excesses measured by GC.
[d] Recycling experiment.

again the nanoparticle catalytic systems provided lower activities and lower enantioselectivities than the corresponding molecular systems (Table 4).

Elucidation of the Nature of the Active Species

Allylic Alkylation

In order to establish the nature of the catalyst, several experiments were carried out using the molecular and nanoparticle catalytic systems. For these experiments we chose **Pd1** and **Pd5** nanoparticles since they show very different catalytic activity (see Table 3). Therefore, while **Pd1** showed low activity (62% conversion after 72 h), **Pd5** was the fastest (100% conversion after 24 h).

TEM and elemental analysis after catalysis: In general, the shape and size distribution of PdNPs is no different from that of the samples before catalysis (Figure 5). This contrasts with the decrease in particle size during the reaction when Pd atoms and/or ions leach from the colloidal clusters as observed by Rothenberg and co-workers.[6d] Although the TEM graphs of the unwashed PdNPs after catalysis have more agglomeration regions (Figure 5b) than the PdNPs before catalysis (Figure 5a), the washed recovered PdNPs had the same degree of agglomerated regions as before catalysis (Figure 5c).[7b] The higher agglomeration degree observed in Figure 5b is probably due to the presence of large amounts of organic material (products and starting compounds) and the ligand leaching from the PdNPs, because of the weak interactions with the metal surface. Moreover, the P and Pd elemental analysis of the recovered nanoparticles after catalysis indicates that the Pd/P ratio is the same as before the catalysis (Pd/P ratio of *ca.* 15/2).[23] This together with no modification in the shape and size distribution of PdNPs during the reaction may suggest that the PdNPs are responsible for the catalytic activity. However, metal leaching cannot be ruled out since Pd(0) molecular species tend to rejoin to the clusters after catalysis as has been shown for the ligand-free Pd-catalyzed Heck reaction at high temperatures.[6a,b]

Kinetic measurements: For the homogeneous molecular systems containing ligands **1** and **5**, the catalyst concentration was decreased in order to obtain reaction rates comparable with those of the nanoparticle ones. We therefore studied the molecular system at different palladium/substrate ratios: 1/500, 1/1,000, 1/5,000 and 1/10,000. For the catalytic systems containing ligand **1**, at Pd/**S1**=1/1,000 and Pd/**S1**=1/5,000, the molecular system (**Mol.1**) was much faster than the nanoparticle one, while the system Pd/**S1**=1/10,000 gave a similar order of magnitude of rate as the **Pd1** one (Figure 6a). However, for the catalytic system containing ligand **5**, the Pd/**S1**=1/500 provided a rate of similar order of magnitude as **Pd5** (Figure 6b). In addition, the kinetic study showed that the reaction rate profiles for **Pd1** and **Pd5** and the corresponding molecular systems, at Pd/**S1**=1/10,000 and Pd/**S1**=1/500, respectively, are similar. Unlike the kinetic resolution observed for other PdNP systems stabilized by chiral non-labile diphosphites,[4] in the present ligand systems substrate **S1** remains almost racemic for both molecular and nanoparticle catalytic systems. This kinetic resolution of substrate **S1** has been one of the main clues to confirm that the PdNPs stabilized by chiral diphosphites are the species truly responsible for the catalytic activity. The catalytic behaviour of the oxazolinyl-phosphite ligand systems may therefore suggest that molecular species leached from the nanoparticles used as catalyst precursors. However, it should be pointed out that for the diphosphite-systems, no control experiments have been done for the molecular catalysts under the same conditions as in the PdNP catalysis (a huge excess of diphosphite and an absence of chloride). Thus, the nature of the active species with our PdNPs remains uncertain.

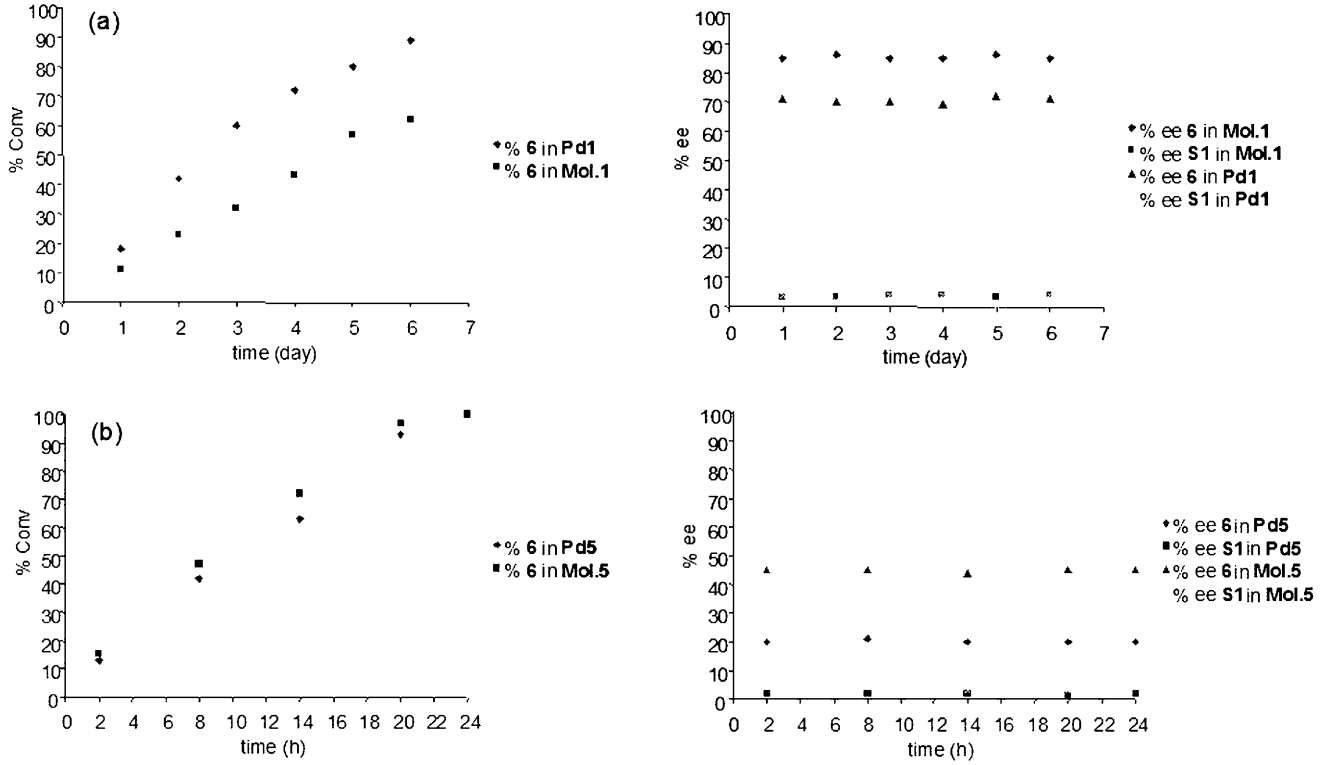

Figure 6. Kinetic profiles for the Pd-catalyzed allylic substitution of **S1**: (a) using **Pd1** and molecular system (**Mol.1**) at **S1**/Pd = 10,000 and (b) using **Pd5** and molecular system (**Mol.5**) at **S1**/Pd = 500.

Poisoning tests: In order to provide further evidence about the nature of the catalyst, we studied the effect of classical poisons (CS_2 and Hg) for both catalysts, molecular and PdNPs. The results are summarized in Table 5 and Table 6. As expected, for the molecular system (**Mol.1** and **Mol.5**) the presence of mercury does not modify the catalytic behaviour, but carbon sulfide decreases the activity of the system. However, the fact that the catalytic reaction stops for the **Pd1** and **Pd5** systems in the presence of either CS_2 or Hg (added after 4 h or 24 h of reaction), seems to indicate the presence of Pd(0) species but they do not provide conclusive evidence about the nature of the active species (nanoparticle or molecular).[6a]

Continuous-flow membrane reactor experiments: For these experiments we used a home-made continuous-flow membrane reactor (see Experimental Section for a more detailed description and set-up of the reactor) equipped with a stirring bar and a membrane placed in the bottom of the reactor (total volume = 6 mL). The reactive solution is pumped through the reactor with a flow rate of 6 mL/h (Figure 7). We

Table 5. Poisoning tests for the asymmetric Pd-catalyzed allylic alkylation of **S1** using **Pd1** and **Mol.1**.

		Nanoparticle precursor **Pd1**[a]			Molecular precursor **Mol.1**[b]		
Entry	Poison	**S1**/**Pd1**/**1**/poison	% Conv.[c] (h)	% *ee* **6**[d]	**S1**/Pd/**1**/poison	% Conv.[c] (h)	% *ee* **6**[d]
1	–	20/1/0.1/–	60 (72)	71 (*S*)	100/1/0.9/–	95 (0.5)	86 (*S*)
2	CS_2[e]	20/1/0.1/0.3	<5 (72)	–	100/1/0.9/1	12 (0.5)	83 (*S*)
3	CS_2[f]	20/1/0.1/0.3	24 (72)	70 (*S*)	100/1/0.9/1	43 (0.5)	85 (*S*)
4	Hg[e]	20/1/0.1/100	<5 (72)	–	100/1/0.9/100	90 (0.5)	85 (*S*)
5	Hg[f]	20/1/0.2/100	45 (72)	70 (*S*)	100/1/0.9/100	93 (0.5)	86 (*S*)

[a] 5 mol% Pd, 0.5 mmol of **S1**, 1.5 mmol of BSA, 1.5 mmol of dimethyl malonate, CH_2Cl_2 as solvent, $T = 23\,°C$.
[b] 0.5 mol% $[PdCl((\eta^3\text{-}C_3H_5)]_2$, 0.9 mol% of **1**, 0.5 mmol of **S1**, 1.5 mmol of BSA, 1.5 mmol of dimethyl malonate, CH_2Cl_2 as solvent, $T = 23\,°C$.
[c] Conversion percentage determined by ^1H NMR.
[d] Enantiomeric excesses determined by HPLC on a Chiralcel-OD column. Absolute configuration shown in parentheses.
[e] Poison added at the beginning of the reaction.
[f] Poison added after 24 h reaction for the colloidal system and after 10 min for the molecular system

Table 6. Poisoning tests for the asymmetric Pd-catalyzed allylic alkylation of **S1** using **Pd5** and **Mol.5**.

		Nanoparticle precursor **Pd5**[a]			Molecular precursor **Mol.5**[b]		
Entry	Poison	**S1**/**Pd5**/**5**/poison	% Conv.[c] (h)	% *ee* **6**[d]	**S1**/Pd/**5**/poison	% Conv.[c] (h)	% *ee* **6**[d]
1	–	20/1/0.1/–	100 (24)	20 (*S*)	100/1/0.9/–	67 (0.5)	45 (*S*)
2	CS_2[e]	20/1/0.1/0.3	<5 (24)	–	100/1/0.9/1	<5 (0.5)	42 (*S*)
3	CS_2[f]	20/1/0.1/0.3	27 (24)	21 (*S*)	100/1/0.9/1	18 (0.5)	43 (*S*)
4	Hg[e]	201/0.1/100	<5 (24)	–	100/1/0.9/100	59 (0.5)	44 (*S*)
5	Hg[f]	20/1/0.2/100	57 (24)	20 (*S*)	100/1/0.9/100	64 (0.5)	45 (*S*)

[a] 5 mol% Pd. 0.5 mmol of **S1**, 1.5 mmol of BSA, 1.5 mmol of dimethyl malonate, CH_2Cl_2 as solvent, $T=23\,^{\circ}C$.
[b] 0.5 mol% $[PdCl((\eta^3\text{-}C_3H_5)]_2$. 0.9 mol% of **5**. 0.5 mmol of **S1**. 1.5 mmol of BSA. 1.5 mmol of dimethyl malonate. CH_2Cl_2 as solvent. $T=23\,^{\circ}C$.
[c] Conversion percentage determined by ^1H NMR.
[d] Enantiomeric excesses determined by HPLC on a Chiralcel-OD column. Absolute configuration shown in parentheses.
[e] Poison added at the beginning of the reaction.
[f] Poison added after 4 h reaction for the colloidal system and after 10 min for the molecular system

used a Koch/SelRO MPF-50 nanofiltration membrane (molecular weight cutoff = 700 Dalton) which is designed to allow the diffusion of leached molecular species, but not of Pd nanoparticles.

Firstly, we studied the alkylation of **S1** using **Pd5**. The membrane, the stirring bar and KOAc were placed at the base of the reactor. They were first flushed with dry dichloromethane overnight and then with a solution containing the substrate **S1**, dimethyl malonate and BSA during 2 h (approx. two reactor volumes). The reaction was started by transferring the catalyst solution (5 mg of **Pd5** and 20 mol% of **5** in 2 mL of dichloromethane) into the membrane reactor. We collected and analyzed the total volume of the solution pumped through the reactor every two reactor volumes. The data are collected in Figure 8. The analysis of the solution collected during the first two reactor volumes pumped through the reactor shows a conversion of 10% with a 19% enantioselectivity. We observed that the catalytic activity stopped after six reactor volumes (Figure 8). To the solution from the first two reactor volumes we added 2 mg of KOAc and allowed this sample to stir for a further 4 h. We observed that conversion increased until 32% while maintaining the same enantioselectivity. This is in agreement with the fact that the active species are molecular complexes that arise from leaching from the nanoparticle. After 8 reactor volumes pumped through, we added to the reactor 10 mol% of ligand in 1 mL of dichloromethane and we observed that the system was again active (6% conversion after 2 reactor volumes, shown also in Figure 8). This clearly indicates that the presence of ligand is necessary to induce the leaching from the PdNPs and therefore exclude the possibility of "naked" molecular Pd(0) species being formed. We also quantified the amount of Pd leached in the solutions coming out of the reactor using ICP-AES. After the first two reactor volumes, 0.6 mg of Pd was found in solution. The molecular system using 0.6 mg of Pd precursor provides a conversion (15% after 2 h, Figure 6b) comparable to that observed for **Pd5** nanoparticle catalysts after two reactor volumes. Therefore, we conclude that the molecular species are the only ones responsible for the catalytic activity. In addition, the lower enantioselectivity achieved using PdNPs compared with those of the molecular system (at L/Pd = 0.9, Table 3) is due to the formation of monomeric molecular Pd-allyl species containing two oxazolinyl-phosphite ligands coordinated in a monodentate fashion through the phosphite moiety, $[Pd(allyl)(\kappa^1\text{-}P\text{-}\mathbf{L})_2]^+$ ($\mathbf{L}=\mathbf{1}$–$\mathbf{5}$). These species have been observed in the molecular system when excess of ligand is present as is the case in the catalysis using PdNP where the resulting ligand-to-metal ratio is high.[24,25]

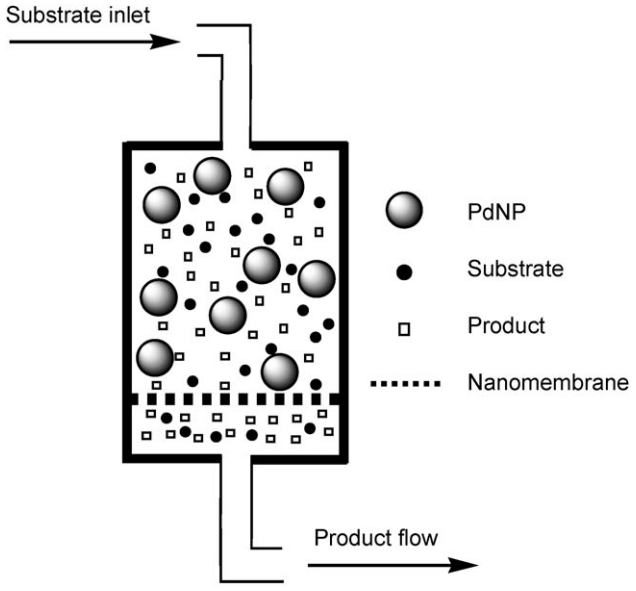

Figure 7. Schematic presentation of a membrane reactor.

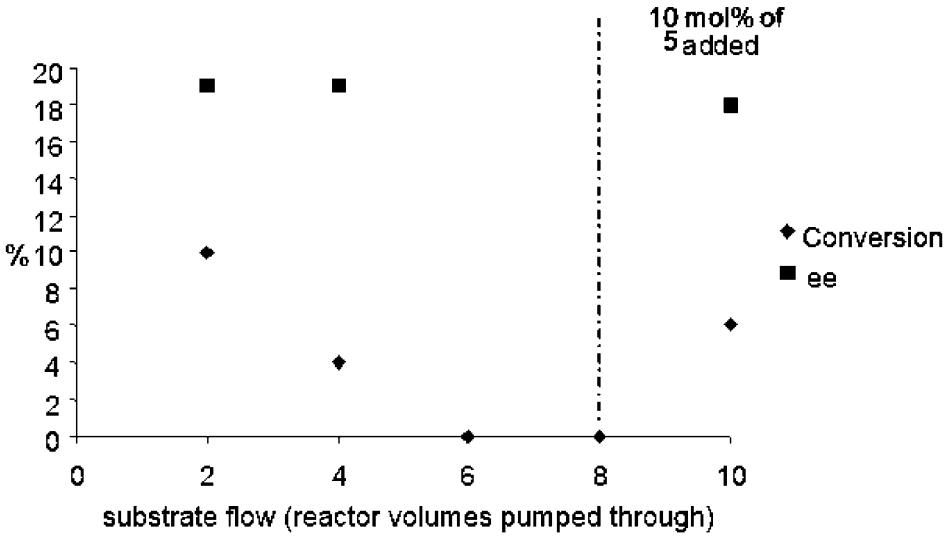

Figure 8. Conversion (◆) and enantioselectivity (■) obtained from the use of **Pd5** in a continuous-flow membrane reactor.

We then studied the alkylation of **S1** using **Pd1**. Since the activity of **Pd1** is lower than that of **Pd5**, we performed the experiment in the membrane reactor but in a different way. After the conditioning of the membrane as previously described, a solution containing all the reactive compounds (**S1**, dimethyl malonate and BSA), **Pd1** and 20 mol% of ligand **1** were placed in the reactor. The reaction mixture was allowed to stir in a batch mode for 2.5 days. After this time, we pumped out the solution of the reactor through the membrane. Analysis of the resulting solution indicated a 63% conversion with an *ee* of 74%. To this sample, we then added 2 mg of KOAc. After 24 h, we observed that conversion increased until 85% maintaining the same enantioselectivity. This clearly shows again that the active species are molecular species that originate from metal leaching from the nanoparticle. The amount of Pd in the filtered sample is 0.06 mg and this fully accounts for the activity if we assume that all the leached Pd atoms form molecular palladium/ligand species.

In summary, the continuous-flow membrane reactor is crucial in the elucidation of the nature of the active species. It proves that the leached molecular palladium species containing oxazolinyl-phosphite ligands are the true catalysts in the Pd-nanocatalyzed allylic alkylation reaction. In addition, this study indicates that the behaviour of the Pd nanoparticles depends on their stability; **Pd1** is more resistant to leaching of molecular species than **Pd5** and therefore the latter is more active.

The previous study on palladium nanoparticles in allylic allylation using diphosphites as the ligands deviated from the molecular catalysts in that kinetic resolution was obtained, which was not observed for the molecular catalyst.[4] The system differs from the present one in that the particles were much larger (4.2 nm, or ~Pd_{3000}) and contained only ~11 diphosphites per cluster (idealized as Pd_{2869}, 9 shells icosahedron, carrying the bulky diphosphites perhaps at the vertices). The enormous excess of ligand in solution can perhaps account for the kinetic resolution observed.

The Asymmetric Heck Reaction

In contrast to the allylic alkylation reaction, the TEM analysis after the reaction shows larger particles than those found in the TEM analysis before the reaction (Figure 9). This indicates that the PdNPs are not stable under the reaction conditions and tend to form larger nanoparticles, probably by ligand loss.[26] In addition, also the poisoning experiments (Table 7) provide conclusive evidence about the nature of the species responsible for the catalytic activity. They agree with a leaching of molecular species being responsible for the catalytic activity. In summary, these experiments in combination with the fact that the nanoparticle system shows the same catalytic trends as the molecular system (Table 4) indicates that our Pd nanoparticles act as a reservoir of molecular species, analogous to that proposed for Heck free-ligand coupling using Pd nanoparticles as catalysts.[6b,9,27] The fact that lower enantioselectivities were achieved using Pd nanoparticles compared with those of the homogeneous system (Table 4) is probably due to the presence of an excess of ligand when using Pd nanoparticles as has been observed for the allylic alkylation reaction.[24]

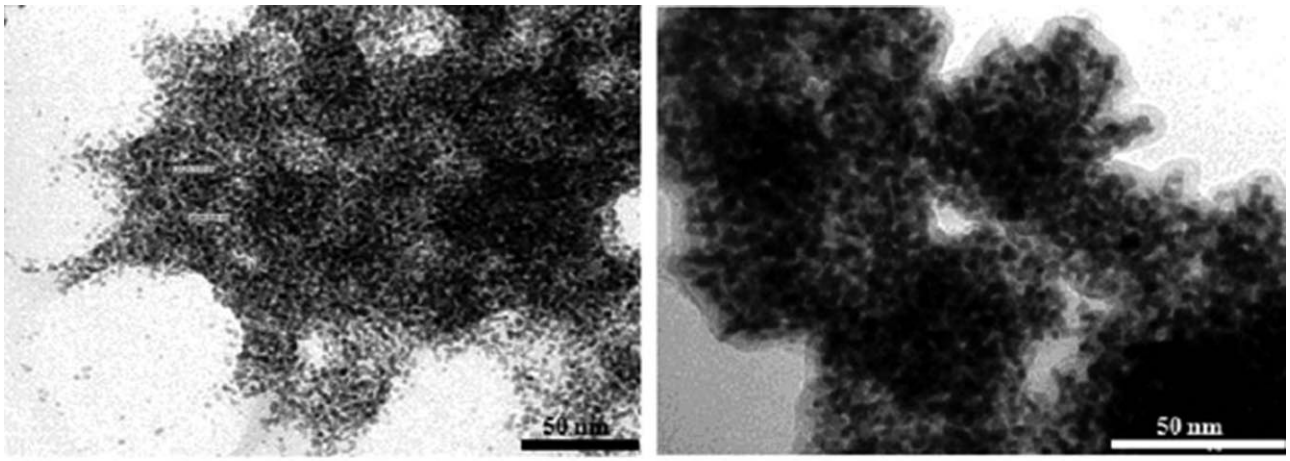

Figure 9. TEM micrographs showing **Pd1** nanoparticles: (a) before and (b) after Pd-catalyzed Heck reaction of **S2**.

Table 7. Poisoning test for the asymmetric Pd-catalyzed phenylation of **S2** using **Pd1** and **Mol.1**.

		Nanoparticle precursor **Pd1**[a,c]				Molecular precursor **Mol.1**[b,c]			
Entry	Poison	**S2**/**Pd1**/**1**/poison	% Conv. (h)	% **7**	% *ee* **7**	**S2**/Pd/**1**/poison	% Conv. (h)	% **7**	% *ee* **7**
1	–	10/1/0.1/–	23 (72)	81	65 (*R*)	40/1/2.2/–	100 (15)	97	99 (*R*)
2	CS_2[d]	10/1/0.1/0.3	<3 (72)	–	–	100/1/0.9/1	21 (24)	97	96 (*R*)
3	CS_2[e]	10/1/0.1/0.3	7 (72)	79	64 (*R*)	100/1/0.9/1	34 (24)	95	96 (*R*)
4	Hg[d]	10/1/0.1/100	<3 (72)	–	–	100/1/0.9/100	87 (24)	95	94 (*R*)
5	Hg[e]	10/1/0.1/100	18 (72)	80	64 (*R*)	100/1/0.9/100	100 (24)	96	97 (*R*)

[a] 10 mol% Pd, 2 mmol of **S2**, 0.5 mmol of PhOTf, 1 mmol of $(i\text{-Pr})_2$NEt, THF as solvent, $T = 50\,^{\circ}C$.
[b] 1.25 mol% of $[Pd_2(dba)_3]$, 2 mmol of **S2**, 0.5 mmol of phenyl triflate, THF as solvent, 1 mmol of $(i\text{-Pr})_2$NEt, $T = 50\,^{\circ}C$.
[c] Conversion percentages and enantiomeric excesses measured by GC.
[d] Poison added in the beginning of the reaction.
[e] Poison added after 24 h reaction for the colloidal system and after 4 h for the molecular system.

Conclusions

We successfully synthesized a series of palladium nanoparticles **Pd1–Pd5** stabilized by five chiral sugar-based oxazolinyl-phosphite ligands, containing several substituents at the oxazoline and phosphite moieties. They were characterized by transmission electron microscopy (TEM), X-ray powder diffraction (XRD), infrared spectroscopy (IR), and elemental analysis. Their structure is akin to that of $[Pd_{561}(OAc)_{180}(L)_{60}]$ (L = phenantroline, bipyridine), analogous to the giant clusters described by Moiseev and co-workers. The new nanoparticles were applied in Pd-catalyzed asymmetric allylic alkylation and Heck coupling reactions. The results obtained by using a continuous-flow membrane reactor (CFMR), TEM, poisoning and kinetic measurements show that the occurrence of monometallic, molecular species can account for the catalytic activity observed. Especially the CFMR experiments proved to be crucial to elucidate that the leached molecular palladium species containing oxazolinyl-phosphite ligands are the actual catalysts. We propose, as in dendrimer catalysis, that CFMR experiments should be conducted routinely to reveal the nature of the catalyst in the liquid phase for catalytic reactions using MNPs. Without further study, our results cannot be extrapolated to other systems. Cross-coupling reactions, however, require three coordination sites at a divalent, hence square-planar, palladium ion – the presence of *ee*s shows that the chiral ligands are coordinated – and it is hard to imagine how a surface atom, even one on the edges, could provide sufficient space to carry out this reaction *via* the commonly accepted mechanism. Nevertheless, the findings can be made useful; when an excess of oxidizing aryl halide is used part of the palladium used will remain in solution, but an excess of nucleophile will result in a palladium(0) complex at the end of the reaction, which could well precipitate on the MNPs, thus facilitating separation.[6e,8,28] Interpretation of such recycling experiments remains tricky though, as it is known that very low concentrations of palladium catalyst can ac-

count for the activity of Suzuki reactions and Heck reactions,[29] and thus the recycling experiments without measurable loss of activity reported frequently are not very informative. For ligand-modified catalysts most likely the most reactive catalyst (precursor) is an arylpalladium halide ligand complex as was shown for the Heck reaction[30] and for the Buchwald–Hartwig N–C cross-coupling reaction, for which turnover frequencies of $140\,h^{-1}$ were obtained at room temperature.[31] Enantioselective catalysis by bulk metal particles surface-modified by chiral additives is an established technique,[32] which remains interesting for MNPs as well, but perhaps one should search for new reactions, more common to metallic catalysts, such as hydrogenation and oxidation,[15,17,33] or reactions less common for molecular species, for example photogeneration of H_2.[34]

Experimental Section

General Considerations

All reactions were carried out under argon using standard Schlenk tube, Fischer–Porter bottle and vacuum line techniques, or in a glove-box. Ligands **1–5** were synthesized as previously described.[10] $[Pd_2(dba)_3]$ was used as commercially available. Solvents were purified and dried by standard procedures. All reagents and solvents were degassed before use by using three freeze-pump-thaw cycles. Elemental analyses were carried out by the "Servei Científic-Tècnics" of the Universitat Rovira i Virgili and by the "Service Central d'Analyses du CNRS" in Lyon.

Synthesis of Palladium Nanoparticles

$[Pd_2(dba)_3{\cdot}CHCl_3]$ (64.7 mg, 0.06 mmol) was dissolved under argon in a solution of THF (50 mL) containing the corresponding ligand (0.0125 mmol) in a closed pressure Fischer–Porter bottle. After pressurization at room temperature under H_2 (3 bar) for 30 min, the initial purple solution became grey in a few minutes. The vigorous magnetic stirring and the pressure of H_2 were maintained for 18 h. The hydrogen pressure was then eliminated, and a drop of the colloidal solution was deposited under argon on a carbon-covered copper grid for microscopy analysis. Evaporation of the solvent gave a black precipitate which was washed with pentane (3×10 mL) and dried at low pressure. The colloids were characterized by TEM, elemental analysis, IR spectroscopy and XRD. **Pd1**: yield: 21 mg, 78%; **Pd2**: yield: 231 mg, 83%; **Pd3**: yield: 20 mg, 64%; **Pd4**: yield: 19 mg, 69%; **Pd5**: yield: 21 mg, 73%.

Procedure for Allylic Alkylation Catalyzed using Palladium Nanoparticles

To a suspension of nanoparticle (5 mg) in dichloromethane (3 mL) the desired amount of the corresponding ligand was added. *rac*-3-Acetoxy-1,3-diphenyl-1-propene (126 mg, 0.5 mmol) and dimethyl malonate (171 μL, 1.5 mmol) dissolved in dichloromethane (2 mL) were then added, followed by BSA (370 μL, 1.5 mmol) and KOAc (2 mg). The mixture was stirred at room temperature and samples were taken off. Each sample was then diluted with diethyl ether (5 mL), filtered over Celite and washed with a saturated aqueous solution of NH_4Cl (3×20 mL) and water (2×20 mL). The organic phase was dried over $MgSO_4$, filtered off, and solvent removed under reduced pressure. The conversion was measured by ^1H NMR. To determine the enantioselectivities by HPLC (Chiralcel-OD, 0.5% 2-propanol/hexane, flow $0.5\,mL\,min^{-1}$), a sample was filtered over basic alumina using dichloromethane as eluent.[35]

Procedure for Allylic Alkylation using Palladium Molecular Systems

A degassed solution of $[PdCl(C_3H_5)]_2$ (0.9 mg, 0.0025 mmol) and the appropriate oxazolinyl-phosphite ligand (0.0055 mmol) in dichloromethane (0.5 mL) was stirred for 30 min. Subsequently, a solution of *rac*-3-acetoxy-1,3-diphenyl-1-propene (126 mg, 0.5 mmol) in dichloromethane (1.5 mL), dimethyl malonate (171 μL, 1.5 mmol), *N,O*-bis-(trimethylsilyl)-acetamide (370 μL, 1.5 mmol) and KOAc (2 mg) were added. The reaction mixture was stirred at room temperature. After the desired reaction time, the reaction mixture was diluted with Et_2O (5 mL) and saturated NH_4Cl (aqueous) (25 mL) was added. The mixture was extracted with Et_2O (3×10 mL) and the extract dried over $MgSO_4$. The solvent was removed and the conversion was measured by ^1H NMR. To determine the enantioselectivities by HPLC (Chiralcel-OD, 0.5% 2-propanol/hexane, flow $0.5\,mL\,min^{-1}$), a sample was filtered over basic alumina using dichloromethane as eluent.[35]

Procedure for Heck Reaction using Palladium Nanoparticles

To a suspension of nanoparticles (10 mg) in THF (5 mL) the desired amount of the corresponding ligand was added. 2,3-Dihydrofuran (151 μL, 2.0 mmol), phenyl triflate (81 μL, 0.50 mmol) and $(i\text{-Pr})_2EtN$ (174 μL, 1.0 mmol) were added to the catalyst solution. The solution was stirred at 50 °C under argon. After the desired reaction time, the mixture was diluted with additional diethyl ether, filtered and washed with water, dried over $MgSO_4$ and evaporated. Conversion and selectivity were determined by GC.[36]

Procedure for Heck Reaction using Palladium Molecular Systems

A mixture of $[Pd_2(dba)_3]$ (12 mg, 1.25×10^{-2} mmol) and the corresponding chiral ligand (2.8×10^{-2} mmol) in dry degassed THF (3.0 mL) was stirred under argon at room temperature for 15 min. 2,3-Dihydrofuran (151 μL, 2.0 mmol), phenyl triflate (81 μL, 0.50 mmol) and $(i\text{-Pr})_2EtN$ (174 μL, 1.0 mmol) were added to the catalyst solution. The solution was stirred at 50 °C under argon. After the desired reaction time, the mixture was diluted with additional diethyl ether and washed with water, dried over $MgSO_4$ and evaporated. Conversion and selectivity were determined by GC.[36]

TEM Analysis

Samples for TEM analysis were prepared in a glove-box by slow evaporation of drops of the colloidal solution deposited onto a carbon-covered copper grid. TEM analyses were performed on a JEOL 1011 electron microscope operating at 100 kV. The size distributions were determined through a manual analysis by measuring 300 particles on a given grid to obtain a statistically size distribution and a mean diameter.

XRD Analysis

Powder X-ray diffraction patterns of the different samples were obtained with a Siemens D5000 diffractometer using nickel-filtered Cu Kα radiation. The patterns were recorded over a range of 2θ angles from 10° to 90° and crystalline phases were identified using the Joint Committee on Powder Diffraction Standards (JCPDS) files.

IR Analysis

IR spectra were recorded on a Perkin–Elmer Spectrometer GX (FT-IR). The samples were prepared by deposition of a drop of concentrated solution onto KBr pellets.

Continuous-Flow Membrane Reactor Experiments

Description of the reactor: A continuous-flow membrane reactor developed previously was used for the elucidation of the nature of the catalytic species. It consists of a stainless steel autoclave in which the catalyst solution can be injected *via* a two-way valve. The membrane is located at the bottom of the autoclave and kept in place by a Viton® O-ring. The Koch/SelRO MPF-50 nanofiltration membrane (MWCO = 700 Dalton)[37] was chosen for the filtration experiments since it has the correct size to allow the diffusion of leached molecular Pd species, but not of Pd nanoparticles.[38] A vessel containing the substrate solution (under inert atmosphere) is connected to the membrane reactor *via* an HPLC pump that pushes the substrate solution into the reactor and through the membrane.

Reactor set-up: A piece of Koch/SelRO MPF-50 membrane (stored in EtOH) was cut to the correct size for the reactor, stored in acetone for one night, and then stored in methanol (for at least one night). After that it was transferred into the membrane reactor. The membrane and KOAc (2 mg) were first flushed overnight with CH_2Cl_2 and then with substrate solution (approximately two reactor volumes, 12 mL). The substrate solution was prepared by mixing **S1** (512 mg, 2 mmol), dimethyl malonate (0.68 mL, 6 mmol) and oBSA (1.48 mL, 6 mmol) in CH_2Cl_2 (60 mL). This solution was pumped through the reactor with a flow rate of 6 mL h^{-1}. The reaction was started by transferring the catalyst solution (5 mg of the corresponding nanoparticle and 20 mol% of ligand in 2 mL of CH_2Cl_2) into the membrane reactor. Samples of the solution coming out of the reactor were collected and analyzed by ^{1}H NMR and HPLC and the palladium content was measured after the appropriate work-up by ICP-AES.[38b,39]

ICP-AES Analysis

The corresponding solution of the reactor volumes pumped through was evaporated under reduced pressure and dissolved in HCl. The ICP-AES measurements were performed with a sequential Jarrell Ash upgraded (Model 25) Atomscan model 2400 ICP scanning monochromator and a Perkin-Elmer Optima 3000 XL instrument. The measured atomic line of Pd was 340.458 nm.

Acknowledgements

We thank Erik Berteling, University of Amsterdam, for his valuable assistance. We thank the Spanish Government [Consolider Ingenio 2010 (Grant CSD2006–0003), CTQ2004–04412/BQU, CTQ2007–62288/BQU and the Ramón y Cajal fellowship to O.P.), the Catalan Government (2005SGR007777, 2006BE00291 to O.P. and Distinction to M.D.), the University of Amsterdam, the Université Paul Sabatier and CNRS for financial support.

References

[1] See, for instance: a) G. Schmid, in: *Nanoparticles, from Theory to Application*, VCH, Weinheim, **2004**; b) G. Schmid, *Chem. Rev.* **1992**, *92*, 1709; c) N. Toshima, T. Yonezawa, *New J. Chem.* **1998**, 1179; d) J. D. Aiken III, R. G. Finke, *J. Mol. Catal. A: Chem.* **1999**, *145*, 1; e) M. A. El-Sayed, *Acc. Chem. Res.* **2001**, *34*, 257; f) H. Bönnemann, R. M. Richards, *Eur. J. Inorg. Chem.* **2001**, 2455; g) D. Astruc, F. Fu, J. R. Aranzaes, *Angew. Chem. Int. Ed.* **2005**, *44*, 7852; h) P. Migowski, J. Dupont, *Chem. Eur. J.* **2007**, *13*, 32.

[2] a) M. Studer, H.-U. Blaser, C. Exner, *Adv. Synth. Catal.* **2003**, *345*, 45; b) H. Bönnemann, G. A. Braun, *Angew. Chem. Int. Ed. Engl.* **1996**, *35*, 1992; c) H. Bönnemann, G. A. Braun, *Chem. Eur. J.* **1997**, *3*, 1200; d) X. Zuo, H. Liu, D. Guo, X. Yang, *Tetrahedron* **1999**, *55*, 7787; e) J. U. Köhler, J. S. Bradley, *Catal. Lett.* **1997**, *45*, 203; f) J. U. Köhler, J. S. Bradley, *Langmuir* **1998**, *14*, 2730.

[3] M. Tamura, H. Fujihara, *J. Am. Chem. Soc.* **2003**, *125*, 15742.

[4] a) S. Jansat, M. Gómez, K. Phillipot, G. Muller, E. Guiu, C. Claver, S. Castillón, B. Chaudret, *J. Am. Chem. Soc.* **2004**, *126*, 1592; b) I. Favier, M. Gómez, G. Muller, M. R. Axet, S. Castillón, C. Claver, S. Jansat, B. Chaudret, K. Philippot, *Adv. Synth. Catal.* **2007**, *349*, 2459.

[5] See for example: a) M. Diéguez, O. Pàmies, C. Claver, *Chem. Rev.* **2004**, *104*, 3189; b) M. Diéguez, O. Pàmies, A. Ruiz, Y. Díaz, S. Castillón, C. Claver, *Coord. Chem. Rev.* **2004**, *248*, 2165; c) M. Diéguez, A. Ruiz, C. Claver, *Dalton Trans.* **2003**, 2957; d) G. J. H. Buisman, M. E. Martin, E. J. Vos, A. Klootwijk, P. C. J. Kamer, P. W. N. M. van Leeuwen, *Tetrahedron: Asymmetry* **1995**, *6*, 719; e) S. C. Gilbertson, C. Chang, *J. Org. Chem.* **1995**, *60*, 6226; f) H. B. Kagan, T. P. Dang, *J. Am. Chem. Soc.* **1972**, *94*, 6429; g) H. Brunner, W. Pieronczyk, *J. Chem. Res. (S)* **1980**, 76; h) T. V. RajanBabu, T. A. Ayers, A. L. Casalnuovo, *J. Am. Chem. Soc.* **1994**,

116, 4101; i) R. Selke, *React. Kinet. Catal. Lett.* **1979**, *10*, 135.

[6] See for instance: a) N. T. S. Phan, M. van der Sluys, C. W. Jones, *Adv. Synth. Catal.* **2006**, *348*, 609; b) J. G. de Vries, *Dalton Trans.* **2006**, 421; c) I. W. Davies, L. Matty, D. L. Hughes, P. J. Reider, *J. Am. Chem. Soc.* **2001**, *123*, 10139; d) M. B. Thathagar, P. J. Kooyman, R. Boerleider, E. Jansen, C. J. Elsevier, G. Rothenberg, *Adv. Synth. Catal.* **2005**, *347*, 1965; e) J. P. Simeone, J. R. Sowa Jr. , *Tetrahedron* **2007**, *63*, 12646; f) G. Budroni, A. Corma, H. Garcia, A. Primo, *J. Catal.* **2007**, *251*, 345; g) D. Astruc, *Inorg. Chem.* **2007**, *46*, 1884; h) J. A. Widegren, R. G. Finke, *J. Mol. Cat. A: Chem.* **2003**, *198*, 317; i) R. Chinchilla, C. Nájera, *Chem. Rev.* **2007**, *107*, 874; j) L. Durán Pachón, G. Rothenberg, *Appl. Organomet. Chem.* **2008**, 288.

[7] The use of reactivity patterns is hampered due to the difficulty to find a reaction that only works with heterogeneous catalysts or *viceversa* (see ref.[6h]). For recent examples, see: a) J. A. Widegren, R. G. Finke, *J. Mol. Catal. A: Chem.* **2003**, *191*, 187; b) S. Jansat, D. Picurelli, K. Pelzer, K. Philippot, M. Gómez, G. Muller, P. Lecante, B. Chaudret, *New J. Chem.* **2006**, *30*, 115.

[8] A. H. M. de Vries, F. J. Parlevliet, L. Schmieder-van de Vondervoort, J. H. M. Mommers, H. J. W. Henderickx, M. A. N. Walet, J. G. de Vries, *Adv. Synth. Catal.* **2002**, *344*, 996.

[9] a) M. B. Thathagar, J. E. ten Elshof, G. Rothenberg, *Angew. Chem. Int. Ed.* **2006**, *45*, 2886; b) A. V. Gaikwad, A. Holuigue, M. B. Thathagar, J. E. ten Elshof, G. Rothenberg, *Chem. Eur. J.* **2007**, *13*, 6908.

[10] a) Y. Mata, O. Pàmies, M. Diéguez, C. Claver, *Adv. Synth. Catal.* **2005**, *347*, 1943; b) Y. Mata, M. Diéguez, O. Pàmies, C. Claver, *Org. Lett.* **2005**, *7*, 5597; c) Y. Mata, O. Pàmies, M. Diéguez, *Chem. Eur. J.* **2007**, *13*, 3296.

[11] Several complexes that may be involved have a molecular mass slightly above 700, but this does not seem to influence the results.

[12] a) D. de Groot, E. B. Eggeling, J. C. de Wilde, H. Kooijman, R. J. van Haaren, A. W. van der Made, A. L. Spek, D. Vogt, J. N. H. Reek, P. C. J. Kamer, P. W. N. M. van Leeuwen, *Chem. Commun.* **1999**, 1623; b) N. J. Hovestad, E. B. Eggeling, H. J. Heidbüchel, J. T. B. H. Jastrzebski, U. Kragl, W. Keim, D. Vogt, G. van Koten, *Angew. Chem. Int. Ed.* **1999**, *38*, 1655; c) N. Brinkmann, D. Giebel, G. Lohmer, M. T. Reetz, U. Kragl, *J. Catal.* **1999**, *183*, 163; d) D. de Groot, B. F. M. de Waal, J. N. H. Reek, A. P. H. J. Schenning, P. C. J. Kamer, E. W. Meijer, P. W. N. M. van Leeuwen, *J. Am. Chem. Soc.* **2001**, *123*, 8453.

[13] a) C. Pan, K. Pelzer, K. Philippot, B. Chaudret, F. Dassenoy, P. Lecante, M.-J. Casanove, *J. Am. Chem. Soc.* **2001**, *123*, 7584; b) K. Philippot, B. Chaudret, *C. R. Chimie* **2003**, *6*, 1019.

[14] a) H. M. Rietveld, *J. Appl. Cryst.* **1969**, *2*, 65; b) C. W. Scheeren, G. Machado, S. R. Teixeira, J. Morais, J. B. Domingos, J. Dupont, *J. Phys. Chem. B.* **2006**, *110*, 13011; c) A. J. Bruss, M. A. Gelesky, G. Machado, J. Dupont, *J. Mol. Cat. A: Chem.* **2006**, *252*, 212.

[15] a) V. V. Volkov, G. van Tendeloo, G. A. Tsirkov, N. V. Cherkashina, M. N. Vargaftik, I. I. Moiseev, V. M. Novotortsev, A. V. Kvit, A. L. Chuvilin, *J. Cryst. Growth* **1996**, *163*, 377; b) M. K. Starchevsky, S. L. Hladiy, Y. A. Pazdersky, M. N. Vargaftik, I. I. Moiseev, *J. Mol. Cat. A: Chem.* **1999**, *146*, 229; c) I. I. Moiseev, M. N. Vargaftik, in: *Perspectives in Catalysis*, (Eds.: K. I. Thomas, K. I. Zamaraev), Blackwell, Oxford, **1992**, pp 91–123; d) V. Y. Shevchenko, M. I. Samoilovich, A. L. Talis, A. E. Madison, *Glass. Phys. Chem.* **2005**, *31*, 259.

[16] Schmid and co-workers have found that usually the ideal icosahedron arrangement is distorted and forms a cubooctahedron geometry. See for instance: a) G. Schmid, M. Harms, J.-O. Malm, J.-O. Bovin, J. van Ruitenbeck, H. W. Zandbergen, W. T. Fu, *J. Am. Chem. Soc.* **1993**, *115*, 2046; b) G. Schmid, B. Morun, J.-O. Malm, *Angew. Chem. Int. Ed. Engl.* **1989**, *28*, 778; c) ref.[1a]

[17] a) M. N. Vargaftik, I. I. Moiseev, D. I. Kochubei, K. I. Zamaraev, *Faraday Discuss.* **1992**, *92*, 13; b) V. P. Oleshko, *J. Mol. Catal. A: Chem.* **2006**, *249*, 4.

[18] This is meant as a rough calculation; also, the clusters are different in nature, as the Moiseev cluster is charged and the present ones contain Pd(0).

[19] For recent reviews on Pd-catalyzed allylic substitution, see: a) J. Tsuji, *Palladium Reagents and Catalysis*, in: *Innovations in Organic Synthesis*, Wiley, New York, **1995**; b) B. M. Trost, D. L. van Vranken, *Chem. Rev.* **1996**, *96*, 395; c) M. Johannsen, K. A. Jorgensen, *Chem. Rev.* **1998**, *98*, 1689; d) A. Pfaltz, M. Lautens, in: *Comprehensive Asymmetric Catalysis*, (Eds.: E. N. Jacobsen, A. Pfaltz, H. Yamamoto), Springer-Verlag, Berlin, **1999**, Vol. 2, Chapter 24; e) B. M. Trost, M. L. Crawley, *Chem. Rev.* **2003**, *103*, 2921; for recent reviews on Pd-catalyzed Heck reactions, see: f) L. F. Tietze, H. Ila, H. P. Bell, *Chem. Rev.* **2004**, *104*, 3453; g) L. X. Dai, T. Tu, S. L. You, W. P. Deng, X. L. Hou, *Acc. Chem. Res.* **2003**, *36*, 659; h) C. Bolm, J. P. Hildebrand, K. Muñiz, N. Hermanns, *Angew. Chem. Int. Ed.* **2001**, *40*, 3284; i) M. Shibasaki, E. M. Vogl, in: *Comprehensive Asymmetric Catalysis*, (Eds.: E. N. Jacobsen, A. Pfaltz, H. Yamamoto), Springer, Heidelberg, **1999**; j) O. Loiseleur, M. Hayashi, M. Keenan, N. Schmees, A. Pfaltz, *J. Organomet. Chem.* **1999**, *576*, 16; k) M. Beller, T. H. Riermeier, G. Stark, in: *Transition Metals for Organic Synthesis*, (Eds.: M. Beller, C. Bolm), Wiley-VCH, Weinheim, **1998**.

[20] B. M. Trost, D. J. Murphy, *Organometallics* **1985**, *4*, 1143.

[21] The recycling was done adding in every run 10 mol% of ligand.

[22] The recycling experiments have been performed following the methodology described in ref.[4a] Therefore, the final catalytic suspension was cooled down to −70 °C to favour the separation of the nanoparticles from the solution. Then, the resulting solution was removed. The remaining solid was washed with dichloromethane under argon and subsequently used as catalyst precursor.

[23] For recovered **Pd1** we found 42.59% of Pd and 2.11% of P. For recovered **Pd5** we found 46.45% of Pd and 1.81% of P.

[24] Y. Mata, *PhD Thesis*, Universitat Rovira i Virgili, **2007**.

[25] The *in situ* NMR study indicates that [Pd(allyl)(κ^1-*P*-**L**)$_2$]$^+$ (**L**=**1**–**5**) are in equilibrium with species [Pd(allyl)(κ^2-*N*,*P*-**L**)]$^+$ (**L**=**1**–**5**) at a ligand-to-palladium ratios higher than 0.9. For example, for ligand **1**: a) at a ligand-to-palladium ratio of 2, 30% of [Pd(allyl)(κ^1-*P*-**1**)$_2$]$^+$ is formed and the *ee* drops to 65%; b) at a ligand-to-palladium ratio of 4, 50% of [Pd(allyl)(κ^1-*P*-**1**)$_2$]$^+$ is formed and the *ee* drops to 38% and c) at a ligand-to-palladium ratio of 0.9, the formation of [Pd(allyl)(κ^1-*P*-**1**)$_2$]$^+$ is not observed.

[26] See, for instance: a) A. Howard, C. E. J. Mitchell, R. G. Egdell, *Surf. Sci.* **2002**, *515*, L504; b) R. Narayanan, M. A. El-Sayed, *J. Am. Chem. Soc.* **2003**, *125*, 8340; c) J. Li, H. C. Zeng, *J. Am. Chem. Soc.* **2007**, *129*, 15839.

[27] C. C. Cassol, A. P. Umpierre, G. Machado, S. I. Wolke, J. Dupont, *J. Am. Chem. Soc.* **2005**, *127*, 3298.

[28] a) R. Najman, J. K. Cho, A. F. Coffey, J. W. Davies, M. Bradley, *Chem. Commun.* **2007**, 5031; b) F. Fernández, B. Cordero, J. Durand, G. Muller, F. Malbosc, Y. Kihn, E. Teuma, M. Gómez, *Dalton Trans.* **2007**, 5572; c) R. Soler, S. Cacchi, G. Fabrizi, G. Forte, L. Martin, S. Martinez, E. Molins, M. Moreno-Manas, F. Petrucci, A. Roig, R. M. Sebastian, A. Vallribera, *Synthesis* **2007**, 3068: d) Y. Zhu, S. C. Peng, A. Emi, Z. Su, Z. Monalisa, R. A. Kemp, *Adv. Synth. Catal.* **2007**, *349*, 1917; e) Y. Tsuji, T. Fujihara, *Inorg. Chem.* **2007**, *46*, 1895; f) M. A. R. Meier, M. Filali, J.-F. Gohy, U. S. Schubert, *J. Mater. Chem.* **2006**, *16*, 3001; g) J. K. Cho, R. Najman, T. W. Dean, O. Ichihara, C. Muller, M. Bradley, *J. Am. Chem. Soc.* **2006**, *128*, 6276.

[29] a) A. Alimardanov, L. Schmieder-van de Vondervoort, A. H. M. de Vries, J. G. de Vries, *Adv. Synth. Catal.* **2004**, *346*, 1812; b) R. B. Bedford, *Chem. Commun.* **2003**, 1787.

[30] G. P. F. van Strijdonck, M. D. K. Boele, P. C. J. Kamer, J. G. De Vries, P. W. N. M. van Leeuwen, *Eur. J. Inorg. Chem.* **1999**, 1073.

[31] a) Y. Guari, G. P. F. van Strijdonck, M. D. K. Boele, J. N. H. Reek, P. C. J. Kamer, P. W. N. M. van Leeuwen, *Chem. Eur. J.* **2001**, *7*, 475; b) Y. Guari, D. S. van Es, J. N. H. Reek, P. C. J. Kamer, P. W. N. M. van Leeuwen, *Tetrahedron Lett.* **1999**, *40*, 3789.

[32] T. Mallat, E. Orglmeister, A. Baiker, *Chem. Rev.* **2007**, *107*, 4863.

[33] R. A. T. M. van Benthem, H. Hiemstra, P. W. N. M. van Leeuwen, J. W. Geus, W. N. Speckamp, *Angew. Chem. Int. Ed.* **1995**, *34*, 457.

[34] N. Toshima, K. Nakata, H. Kitoh, *Inorg. Chim. Acta* **1997**, *265*, 149.

[35] O. Pàmies, G. P. F. van Strijdonck, M. Diéguez, S. Deerenberg, G. Net, A. Ruiz, C. Claver, P. C. J. Kamer, P. W. N. M. van Leeuwen, *J. Org. Chem.* **2001**, *66*, 8867.

[36] S. R. Gilbertson, Z. Fu, *Org. Lett.* **2001**, *3*, 161.

[37] a) Koch Membrane Systems, Wilmington, USA, http://www.kochmembrane.com; b) C. Linder, M. Nemas, M. Perry, R. Katraro, U. S. Patent 5,265,734, **1992**.

[38] This set-up has previously given good results with dendritic ligands in transition metal catalysed reactions. See, for instance ref.[9a] and: a) D. de Groot, P. G. Emmerink, C. Coucke, J. N. H. Reek, P. C. J. Kamer, P. W. N. M. van Leeuwen, *Inorg. Chem. Commun.* **2000**, *3*, 711; b) D. de Groot, J. N. H. Reek, P. C. J. Kamer, P. W. N. M. van Leeuwen, *Eur. J. Org. Chem.* **2002**, 1085; c) J. N. H. Reek, D. de Groot, G. E. Oosterom, R. van Heerbeek, P. C. J. Kamer, P. W. N. M. van Leeuwen, *Polym. Mater. Sci. Eng.* **2001**, *84*, 158; d) G. E. Oosterom, S. Steffens, J. N. H. Reek, P. C. J. Kamer, P. W. N. M. van Leeuwen, *Top. Catal.* **2002**, *19*, 61.

[39] A. Buhling, J. W. Elgersma, S. Nkrumah, P. C. J. Kamer, P. W. N. M. van Leeuwen, *J. Chem. Soc., Dalton Trans.* 1996, 2143.

